Structure and Paramyosin Content of Tarantula Thick Filaments

RHEA J. C. LEVINE, ROBERT W. KENSLER, MARY C. REEDY,*
WALTRAUD HOFMANN,‡ and HARRIET A. KING
Department of Anatomy, The Medical College of Pennsylvania, Philadelphia, Pennsylvania 19129;
**Department of Anatomy, Duke University Medical Center, Durham, North Carolina 27710; and*
‡Department of Biophysics, The Max-Planck Institute for Medical Research, Heidelberg, Federal Republic of Germany

ABSTRACT Muscle fibers of the tarantula femur exhibit structural and biochemical characteristics similar to those of other long-sarcomere invertebrate muscles, having long A-bands and long thick filaments. 9–12 thin filaments surround each thick filament. Tarantula muscle has a paramyosin:myosin heavy chain molecular ratio of 0.31 ± 0.079 SD. We studied the myosin cross-bridge arrangement on the surface of tarantula thick filaments on isolated, negatively stained, and unidirectionally metal-shadowed specimens by electron microscopy and optical diffraction and filtering and found it to be similar to that previously described for the thick filaments of muscle of the closely related chelicerate arthropod, *Limulus*. Cross-bridges are disposed in a four-stranded right-handed helical arrangement, with 14.5-nm axial spacing between successive levels of four bridges, and a helical repeat period every 43.5 nm. The orientation of cross-bridges on the surface of tarantula filaments is also likely to be very similar to that on *Limulus* filaments as suggested by the similarity between filtered images of the two types of filaments and the radial distance of the centers of mass of the cross-bridges from the surfaces of both types of filaments. Tarantula filaments, however, have smaller diameters than *Limulus* filaments, contain less paramyosin, and display structure that probably reflects the organization of the filament backbone which is not as apparent in images of *Limulus* filaments. We suggest that the similarities between *Limulus* and tarantula thick filaments may be governed, in part, by the close evolutionary relationship of the two species.

Using a modified isolation procedure and improved electron microscopic techniques together with computer image and optical diffraction analyses, we recently described the structure of the myosin cross-bridge arrangement on the surface of negatively stained thick filaments isolated from unstimulated *Limulus* telson levator muscle (15, 22, 30). Four cross-bridges extend from the surface of these filaments at each level, with an axial rise of 14.5 nm between adjacent levels and a helical repeat period of 43.5 nm, as predicted by Wray et al. (36) and confirmed by computer image reconstruction (30). Furthermore, by unidirectional metal-shadowing we determined that the myosin cross-bridges are disposed in a major right-handed helix, having 12 subunits per complete turn (175 nm), on the filament surface (16).

Wray (35) recently reported that the x ray patterns from glycerinated, relaxed tarantula leg muscle resemble those he earlier obtained from similar preparations of *Limulus* muscle (36). Here we present the results of an electron microscopic, optical diffraction, and biochemical analysis of the structure and paramyosin content, respectively, of thick filaments from tarantula femur muscle fibers and compare them with those from our previous analysis of *Limulus* telson muscle thick filaments (15, 16, 22, 30).

MATERIALS AND METHODS

Tarantula (*Eurypelma* sp.) specimens (sex unknown) were purchased from Carolina Biological Supply Co. (Burlington, NC). The spiders were cooled to promote torpor either by surrounding them with ice for an hour, or by placing them in the freezer at −4°C for 20 min, and the legs were removed. The femur (with patella and coxa attached) was cut loose and slit lengthwise to expose the muscles which were dissected according to Dillon (7). All femur muscles were used.

THE JOURNAL OF CELL BIOLOGY · VOLUME 97 JULY 1983 186–195

Electron Microscopy: For sectioned material, live muscles were fixed at body length, in situ with 2.5% glutaraldehyde (Tousimis) and 0.1% tannic acid (Mallinckrodt Inc., Science Products Div., St. Louis, MO) in 20 mM MES (2, [*N*-morpholino] ethanesulfonic acid) (Calbiochem-Behring Corp., San Diego, CA) buffer, 10 mM $MgCl_2$, 5 mM NaN_3, pH 6.8, 4°C for 1 h. Bundles were dissected free in 20 mM MES buffer, pH 6.8, and postfixed in 1% osmium tetroxide in 0.1 M phosphate buffer, 10 mM $MgCl_2$, pH 6.8, 4°C for 30 min, rinsed in water and stained en bloc with 1% uranyl acetate for 2 h at room temperature. Specimens were dehydrated, infiltrated, embedded in Araldite 506 (CIBA-Geigy Chemical Co.) (25), and sectioned on a Reichert OMU-3 ultramicrotome with a Diatome knife. Bronze-to-grey sections on thin carbon films were stained with 2% aqueous potassium permanganate (26) and alkaline lead (25, 27).

Thick filaments were isolated from freshly dissected leg muscle, according to our previously published technique (15), adsorbed onto thin carbon films on electron microscope grids, and negatively stained with 1% aqueous uranyl acetate. In some preparations, the filaments on the grids were washed with several drops of 0.1% Bacitracin (Sigma Chemical Co., St. Louis, MO), prior to negative staining (11). Shadowing of isolated filaments on grids was performed according to our previously reported method (16). In the case of shadowed material, precautions were taken to insure proper orientation of the specimen with respect to insertion of the grid for electron microscopy and orientation of the negatives for reversal negative-making and final printing, as previously described (16), in order to maintain the true direction of the surface helix. Electron micrographs were taken at nominal magnifications of 10,000, 20,000, and 70,000, at 80 kV on either a Siemens 101 or Philips EM 300 electron microscope. Catalase crystals (38) were photographed to calibrate the electron-optical magnifications.

Measurements of sarcomere and A-band lengths were made from electron micrographs of longitudinally sectioned muscle. Thick-filament diameters were measured both on electron micrographs of cross-sectioned muscle and on high magnification electron micrographs of negatively stained filaments. Filament lengths were measured on electron micrographs of unidirectionally shadowed isolated filaments.

Optical Diffraction: Original electron micrograph negatives were diffracted according to standard techniques using a helium-neon laser (Spectra-Physics Inc., Mountain View, CA), operating at 632.8 nm wave length, as the light source. Diffraction patterns were recorded on either 35 mm film or Polaroid type 55 P/N sheet film. Layer-line spacings and positions of primary and subsidiary maxima were measured and computed as previously described (15). In most cases, the spacings on the transforms were calculated relative to the spacing of the third layer line (first meridional reflection) at 1/14.5 nm^{-1}. Filtered images were obtained from some original negatives according to Erickson et al. (10), using their method for preparing aluminum foil masks. A 200-μm diameter punch was used to make slits extending over the full extent of all the layer lines visible in Fig. 2*c*. The first (1/43.8 nm^{-1}) layer line extended out to a radius of ~1/7.2 nm^{-1}, the second and fourth layer lines somewhat less. The third 1/14.5 nm^{-1} and sixth meridionals and layer lines were punched, but in the particular image used in Fig. 5*a* no intensity was detectable on the fifth layer line and no slit was punched in the mask. This was done because the fifth layer line was always extremely weak or absent in all optical diffraction patterns and made no detectable contribution to the image, but the slit in the mask selected out Fourier components with that periodicity from the background and laid them at random over the entire image (10). Averaging occurred over ~130–140 nm. The equator was not included in the mask of the image shown in Fig. 5*a*, so that the muscle transform spikes were not included; the edge of the filament is therefore indistinct.

Quantitative SDS PAGE: For determination of paramyosin:myosin heavy chain molecular ratios (PM:MHC), freshly dissected tarantula leg muscle was glycerinated and stored at −18°C for 3 wk prior to use (8). Myofibrillar homogenates at different protein concentrations (4.1–22.5 μg total protein in 20-μl sample buffer) were prepared for quantitative SDS polyacrylamide disc gel electrophoresis (SDS PAGE) (32) from both glycerinated tarantula leg and *Limulus* telson muscles as previously described (21). In a separate experiment to identify the paramyosin band on both *Limulus* and tarantula gels, purified *Limulus* paramyosin (LPM 1–4 μg) was co-electrophoresed with 10–20 μg loadings of both *Limulus* and tarantula myofibrillar homogenates, respectively, on slab gels, according to Laemmli (18). The gels were scanned at 580 nm on an ISCO Model 1310 gel scanner and Model OA-5 absorbance transmitter (Instrumentation Specialities Co.). Scans were traced on a Kipp and Zonen BD 12 recorder, and the areas under the peaks were measured by planimetry using an electronic graphics calculator (Numonics Corp., Lansdale, PA). The PM:MHC dye binding ratios were averaged from the integration of 61 tarantula and 62 *Limulus* gels, and the PM:MHC molecular ratios were calculated as previously described (21). The *Limulus* gels were used as system controls, since we had previously reported the PM:MHC ratio for this muscle (21).

RESULTS

Electron Microscopy of Sectioned Muscle

We found that the myofibrillar and myofilamentous organization of tarantula femur muscle fibers is essentially identical to that described for four different tarantula leg muscles (39), tarantula tarsal claw depressor muscle (29), and the femoral flexor of the spider *Heteropoda venetoria L.* (14) and closely resembles that of other "long-sarcomere" invertebrate striated muscles (4, 5, 8).

All regions of the sarcomere appear sequentially within each myofibril in single cross-sections (Fig. 1*b*). This probably reflects the skewed orientation of the sarcomeres, which is common to such long-sarcomere fibers (8). In cross-section (Fig. 1), it is also apparent that the sarcomeres in muscle fixed at body length are at complete filament overlap. There are very narrow areas which contain only thin-filament profiles (I-bands) and no regions which contain only thick-filament profiles (H-zones). There is no evidence of double overlap of thin filaments, however, since everywhere in the A-band each thick filament is surrounded by a rosette of nine to twelve thins (Fig. 1, *a–c*).

The thick filaments themselves appear approximately circular in cross-section and are disposed in an irregular hexagonal lattice which becomes increasingly regular at the ends of the A-bands, where thick-filament profiles are seen in proximity to the Z-line material (Fig. 1*b*). While tarantula thick filaments do not appear "hollow" as do the thick filaments of many other arthropid muscles, notably insect and crustacean muscles (20, 23, 27), they do exhibit slightly decreased electron density at their cores. The filament cortices are very electron-dense and a cloud of moderately electron-dense material, presumably cross-bridges, extends from the thick-filament surfaces toward the surrounding thin filaments (Fig. 1*c*). The mean diameter of 215 thick filaments, measured on such high magnification micrographs, is 20.2 ± SD 0.45 nm.

The complete overlap of thin and thick filaments in sarcomeres of tarantula fibers fixed at "body length" is also visible in longitudinal sections. The sarcomeres are ~5 μm in length with very narrow I-bands. Although the length of individual thick filaments could not be measured accurately in longitudinally sectioned fibers, A-bands range between 4 and 4.7 μm in length with no visible H-zones (Fig. 1*d*).

Although we did not study the membrane systems of the fibers comprehensively, our observations agree with previously published studies of spider long-sarcomere muscles (14, 29, 39).

Electron Microscopy of Isolated Thick Filaments

Thick-filament length is best determined in both negatively stained and metal-shadowed preparations of isolated filaments. Only those filaments with central bare zones and tapered ends were measured. As suggested by the length of the A-band in longitudinally sectioned muscle fibers, and as expected for a long-sarcomere muscle, tarantula thick filaments are long, with an average length for isolated filaments of 4.2 ± SD 0.31 μm (n = 92).

Negatively Stained Isolated Thick Filaments

In negatively stained preparations (Fig. 2, *a* and *b*), the thick filaments show bipolar symmetry on either side of the prom-

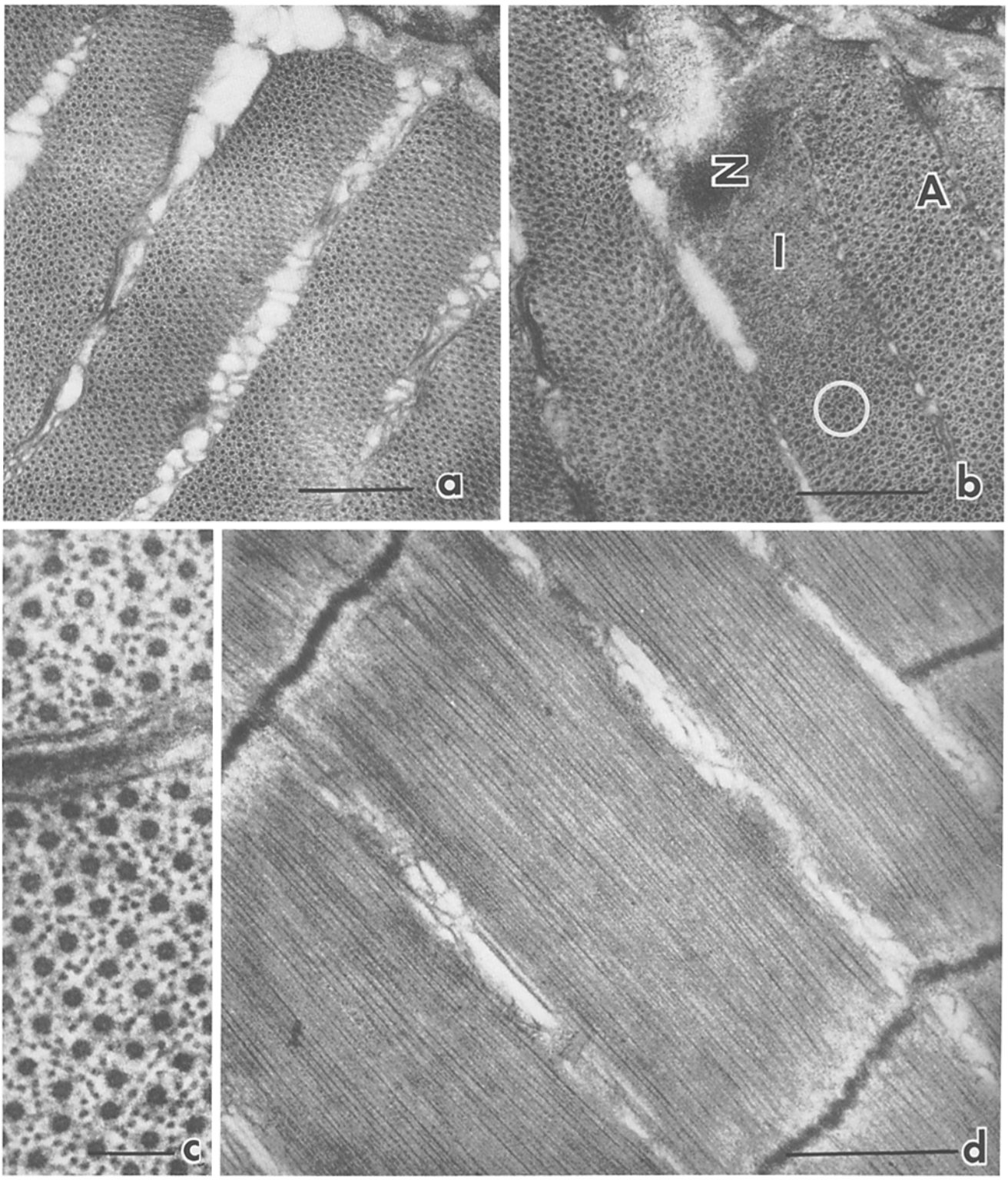

FIGURE 1 Electron micrographs of sections of fresh-fixed tarantula leg muscle fibers. (*a*, *b*, and *c*) Cross sections. Note the strap-like myofibrillar shape in *a* and *b*. (a) Bar, 0.5 μm. × 41,000. (*b*) (*A*) A band. (*I*) I band. (*Z*) Z line. Note the regular hexagonal array of thick filaments near the end of the A band, especially evident within the white circle. Bar, 0.5 μm. × 46,500. (c) High magnification image of the filament lattice. Note the paler appearance of the centers of the thick filaments, and the rosettes of 9–12 thin filaments surrounding each thick filament. Bar, 100 nm. × 150,000. (*d*) Longitudinal section showing complete overlap of the thick and thin filaments (no H band) in this ~4.5 μm sarcomere. Bar, 1.0 μm. × 30,000.

inent, central bare zone. They are strikingly periodic, with the surface structure repeating at ~43 nm. The surface periodicity of tarantula thick filaments is remarkably similar to that reported for *Limulus* thick filaments with respect to both the overall pattern of stain-excluding structures, presumably myosin cross-bridges, and the symmetrical disposition of these on either side of the filaments' central longitudinal axes (17, 22). At high magnification it is apparent that the pattern on

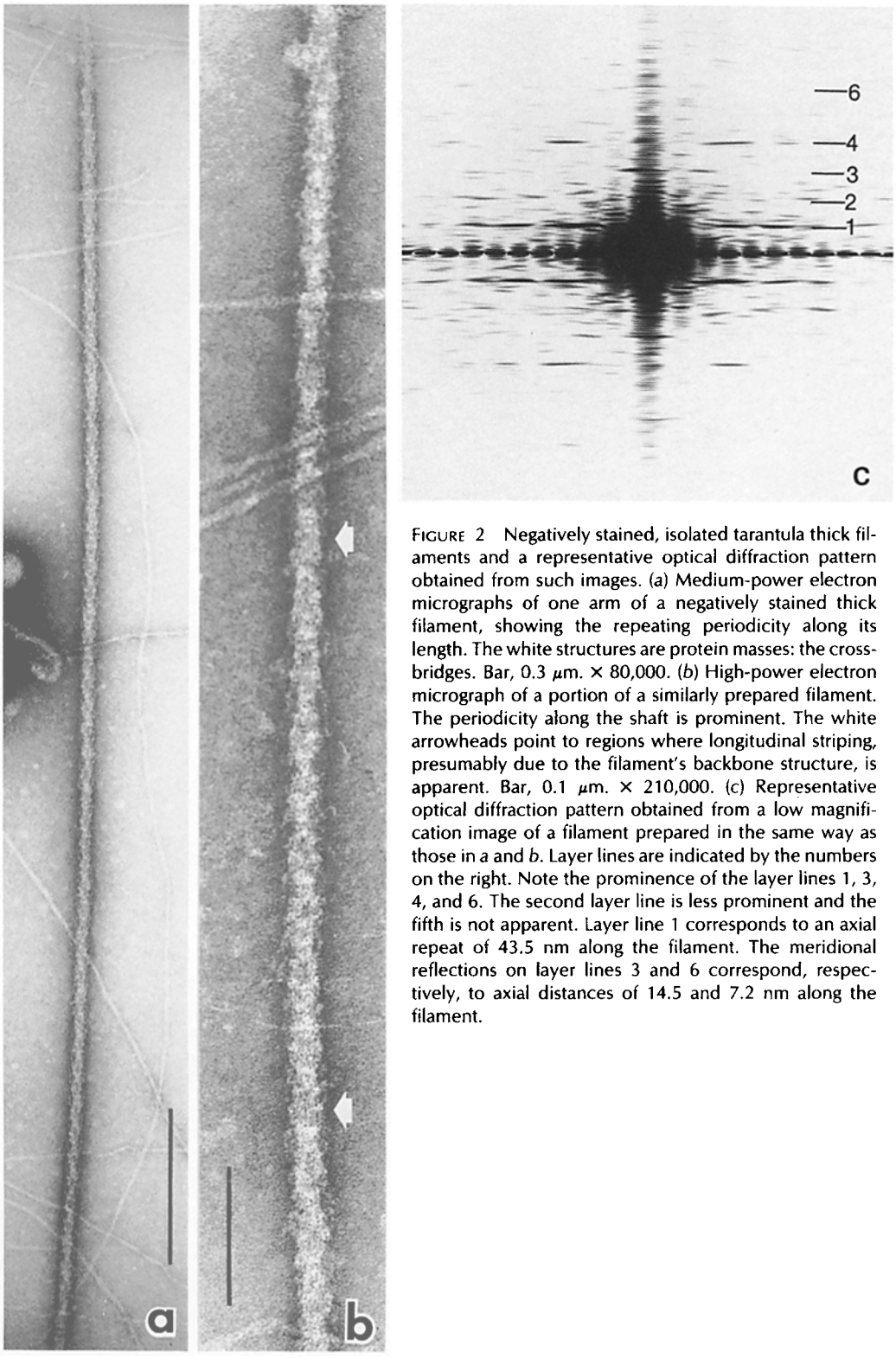

FIGURE 2 Negatively stained, isolated tarantula thick filaments and a representative optical diffraction pattern obtained from such images. (a) Medium-power electron micrographs of one arm of a negatively stained thick filament, showing the repeating periodicity along its length. The white structures are protein masses: the cross-bridges. Bar, 0.3 μm. × 80,000. (*b*) High-power electron micrograph of a portion of a similarly prepared filament. The periodicity along the shaft is prominent. The white arrowheads point to regions where longitudinal striping, presumably due to the filament's backbone structure, is apparent. Bar, 0.1 μm. × 210,000. (c) Representative optical diffraction pattern obtained from a low magnification image of a filament prepared in the same way as those in *a* and *b*. Layer lines are indicated by the numbers on the right. Note the prominence of the layer lines 1, 3, 4, and 6. The second layer line is less prominent and the fifth is not apparent. Layer line 1 corresponds to an axial repeat of 43.5 nm along the filament. The meridional reflections on layer lines 3 and 6 correspond, respectively, to axial distances of 14.5 and 7.2 nm along the filament.

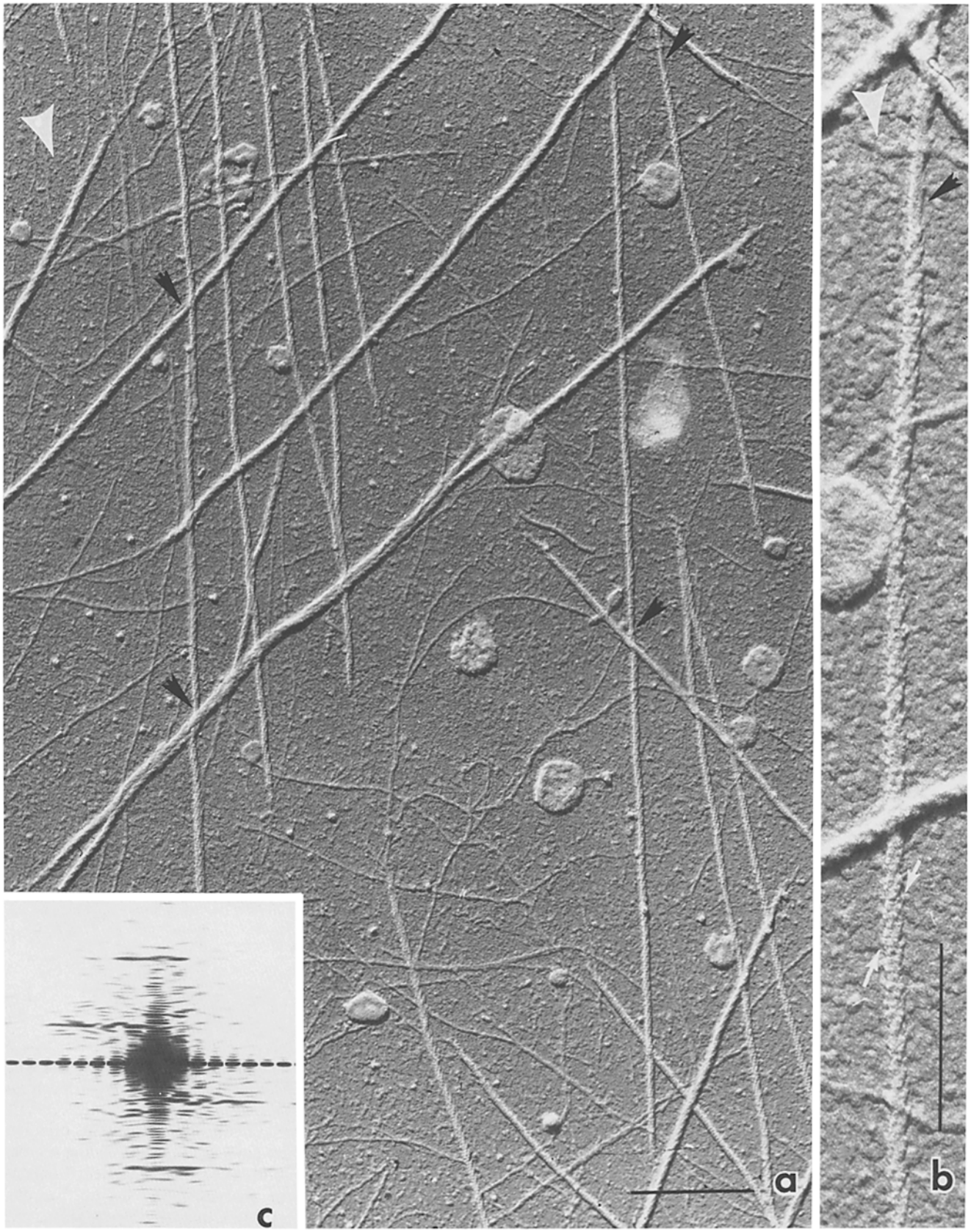

FIGURE 3 Images of unidirectionally metal-shadowed thick filaments isolated from tarantula leg muscle. In both *a* and *b*, the large white arrowheads indicate the direction of shadowing. (a) Medium-power electron micrograph showing a field of isolated, shadowed filaments. A major right-handed helix is present on all filaments. Note the difference in appearance of the filament surface depending upon its position in relation to the shadowing source. Bare zones are indicated by black arrowheads. Bar, 0.5 μm. × 48,000. (*b*) High-power electron micrograph of a filament (present in the upper right-hand corner of *a*) oriented almost parallel to the direction of shadowing. The bare zone is indicated by the black arrowhead. Note the knoblike appearance of the surface subunits, presumably cross-bridges, which are arranged along a major right-handed helix that repeats axially every 43.5 nm. Six subunits are visible along each helical strand on the surface facing the viewer (white arrowheads). Bar, 0.3 μm. × 115,000. (c) Optical diffraction pattern from a shadowed filament. Note the persistence of the layer lines, despite the one-sided appearance of the transform.

tarantula thick filaments also repeats at every third level of cross-bridges (Fig. 2*b*). Interestingly, as suggested by Wray (35) from x ray diffraction studies, tarantula thick filaments appear to show more backbone detail than do *Limulus* filaments. This backbone structure is seen as longitudinal striping of stain-excluding structure, running nearly parallel to the filaments' long axes (Fig. 2*b*). The diameter of the filament at the bare zone is ~19–20 nm as measured on images at high magnification, while the centers of the cross-bridge mass measure at a diameter of ~28 nm.

Metal-shadowed Isolated Thick Filaments

When unidirectionally shadowed with either platinum or platinum-carbon, tarantula filaments oriented nearly perpendicular to the shadowing source exhibit a ropelike surface structure, with a separation of ~43 nm axially between adjacent right-handed helical strands (Fig. 3). Filaments oriented more nearly parallel to the shadowing source have a knobbier surface, due to the outlining of individual surface subunits, presumably the cross-bridge regions of the myosin molecules (16, 22), by the deposited metal (Fig. 3*b*). Each half-turn of each helical strand is composed of at least six such subunits. Occasionally, there is evidence of a seventh subunit, but never are more than seven nor fewer than six visible.

Optical Diffraction

Electron micrographs of both negatively stained and metal-shadowed tarantula thick filaments produce strong optical diffraction patterns (Fig. 2*c*). Meridional reflections occur at 1/14.5 and 1/7.3 nm^{-1} and occasionally as far out as 1/4.8 nm^{-1}. The transform in Fig. 2*c* does not extend out this far. In many transforms from negatively stained filaments, moderately strong subsidiary maxima are seen to be associated with the 1/14.5 nm^{-1} meridional reflection. Off-meridional reflections produce layer-lines which index close to the first, second, fourth, fifth and occasionally seventh order of a 43.5-nm helical repeat (Tables I and II). Reflections on the first and fourth layer lines are more intense than those on the second and fifth layer lines. Equatorial reflections are present at ~1/11.0–1/12.0 nm^{-1} and ~1/6.0 nm^{-1}. Using the argument $2\pi rR = 3.8$ to describe the position of the secondary peak of the zero-order Bessel function, J_o, which describes the third layer line, and the measured radial spacing (R in the above equation) of these subsidiary maxima: 1/22.1 nm^{-1}, (12, 37), we calculated that the cross-bridges were centered at a radius (r in the above equation) of 13.4 nm. Since the radial position of the primary peak on the first layer line is related to both the radial position of the cross-bridges and the number of strands on the myosin helix (12, 37), we estimated the rotational symmetry of the filaments using the calculated value (r = 13.4 nm) for the radial position of the center of the cross-bridge mass and the measured radial position of the primary maxima on the first layer line (R = 1/15.8 nm^{-1}) in the argument $2\pi rR = J_n$, where J_n is the Bessel function describing the position of the primary maxima on the first layer line. Our calculated value: 5.33 is extremely close to the expected maximum of 5.32 for a J_4 Bessel function, indicating the extremely high probability of a rotational symmetry of four for the myosin helix on tarantula thick filaments (Tables I and II).

As expected, optical transforms obtained from shadowed filaments are qualitatively very similar to those from negatively stained preparations but are dominated by reflections arising from only one side of the helical array of myosin cross-bridges (Fig. 3*c*) (16, 22). The most detailed transforms of shadowed preparations are obtained from filaments oriented with their long axes nearly parallel to the shadowing source, since these display cross-bridge structure in greatest detail.

Thus, optical diffraction analysis of electron micrographs of both negatively stained and unidirectionally shadowed tarantula thick filaments supports the visual interpretation of the cross-bridge arrangement of these structures as a four start helix with each chain consisting of 12 cross-bridges per turn. There are four cross-bridges at each 14.5 nm axial level (or crown) and the threefold screw symmetry produces an axial repeat at every third cross-bridge level (43.5 nm).

TABLE I

Measurements of Maxima

	Tarantula		*Limulus**	
	Mean ± SD ($1/nm^{-1}$)	n‡	Mean ± SD ($1/nm^{-1}$)	n‡
Layer line spacings				
Layer lines (LL)				
1	43.1 ± 1.4	15	43.2 ± 1.4	49
2	21.9 ± 0.7	14	22.1 ± 0.4	49
3	14.5§	§	14.6 ± 0.1	49
4	10.9 ± 0.2	16	10.9 ± 0.1	49
5	8.7 ± 0.2	7	8.8 ± 0.1	15
6	7.2 ± 0.1	14	7.3 ± 0.1	19
Radial spacings of diffraction maxima				
Maxima				
Primary on first LL	15.7 ± 1.8	16	17.8 ± 1.8	49
Primary on fourth LL	15.8 ± 1.5	16	18.2 ± 2.1	49
First subsidiary on third LL	22.1 ± 3.5	6	25.7 ± 2.6	39

Measurements of maxima on diffraction patterns obtained from negatively stained tarantula thick filaments and a comparison of these data with those previously obtained from *Limulus* thick filaments. Calculations of the cross-bridge radius and Bessel functions describing the position of the primary maxima on the first line of the two thick filaments are also given (Table II).

* Previously published data (13).

‡ Number of diffraction patterns measured.

§ All tarantula measurements were normalized to 1/14.5 nm^{-1} spacing for meridional reflections on third LL.

TABLE II

Measurements of Maxima

	Tarantula	*Limulus**	Table values		
Calculated cross-bridge radius					
Based on first subsidiary maxima on the third LL	13.4	15.5			
Comparison of calculated maxima ($2\pi rR$)*					
Measurements used			J_3	J_4	J_5
Calculated radius of cross-bridges and calculated radial spacings of maxima on first LL	5.36	5.5	4.2	5.32	6.4

* For Bessel Function describing position of primary maxima on first layer line and table values

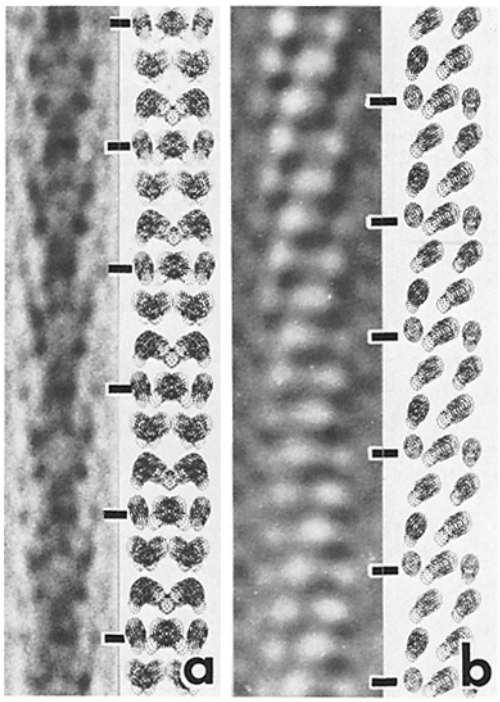

FIGURE 4 Comparison of optically filtered images of negatively stained and platinum-carbon shadowed tarantula thick filaments with computed models of the cross-bridge arrangement on *Limulus* thick filaments. (*a*) Optical filtration of negatively stained tarantula thick filament and computed model of *Limulus* thick filament at 0° rotation. Dark regions represent the mass of the cross-bridges and both surfaces of the filaments are included. (*b*) Optical filtration of platinum-carbon-shadowed tarantula thick filament and computed model of cross-bridge arrangement on one surface of *Limulus* thick filament, showing helical path of each strand in these four-stranded structures. Subunits (knobs) on the filtered image represent cross-bridges, which are arranged in a fairly similar fashion on both filaments. It should be noted that subtle differences that may exist between the cross-bridge arrangements on the surfaces of tarantula and *Limulus* filaments are not detectable at the level of resolution attained here. Nevertheless, the threefold screw symmetry and the rotational symmetry of four (4-strandedness) that is common to both of these filaments is readily apparent. In both *a* and *b*, levels of 43.5 nm on each filtered image and its paired model are connected by lines.

Optical Filtration

Optical filtration was performed on original electron micrograph negatives of negatively stained and shadowed thick filaments. In Fig. 4, the appearance of the cross-bridge array in the filtered images is compared with models for the *Limulus* filament. The great similarity in structure of the two types of thick filaments is readily apparent. The filtered image of the negatively stained tarantula thick filament resembles the view of the *Limulus* model seen in Fig. 4*a* of Kensler and Levine (15) while the filtered image of the platinum-carbon shadowed tarantula filament shows a subunit arrangement similar to the one-sided model. Of particular interest is the observation that the angles between subunits and filament axis in the filtered images of tarantula filaments are similar to the cross-bridge angles apparent on computed reconstructions of *Limulus* filaments (30).

Quantitative SDS PAGE

SDS gels of myofibrillar homogenates of tarantula leg muscle show a band at ~112,000 daltons which appears to be

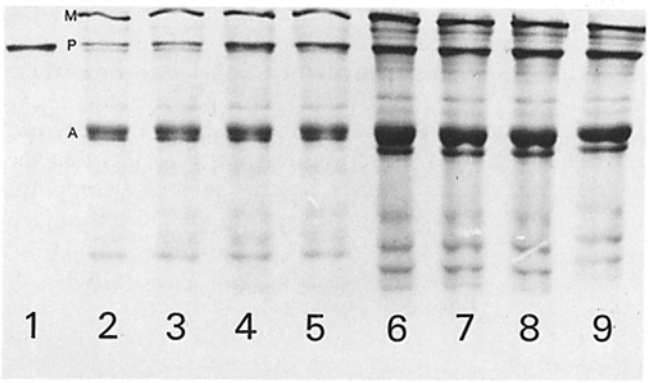

FIGURE 5 SDS PAGE slab gel of purified *Limulus* paramyosin (LPM) electrophoresed alone and together with myofibrillar homogenates of glycerinated *limulus* telson muscle (L) and tarantula leg muscle (T). (*M*) Myosin heavy chain band. (*P*) Paramyosin band. (*A*) Actin band. Lane *1* contains LPM (5 μg) alone. Lane *2* contains LPM (10 μg), alone. Lanes *3*, *4*, and *5* contain 10 μg each, T, plus added LPM (1, 2, and 4 μg, respectively.). Lane 6 contains L (20 μg), alone. Lanes *7*, *8*, and *9* contain 20 μg L, each, plus added LPM (1, 2, and 4 μg, respectively). Note that the LPM comigrates on gels with the paramyosin band in homogenates of tarantula as well as *Limulus* muscle.

TABLE III
Comparisons of Data

Measured and calculated values	Tarantula		*Limulus*	
	Mean ± SD	*n**	Mean ± SD	*n**
Thick filament diameter (nm)				
In situ cross-sections (overlap zone)	20.2 ± 0.45	215	24.6 ± 1.6‡	111‡
Isolated, negatively stained (bare zone)	19–20	5	23.4 ± 1.3§	36§
Calculated value for distance of greatest cross-bridge mass from filament shaft (nm)	3.5–4		4§	
Thick filament length (μm) (isolated, negatively stained)	4.2 ± 0.31	92	4.1 ± 0.2§	100§
Paramyosin:myosin heavy chain (myofibrillar homogenates on SDS PAGE)	0.31 ± 0.079	61	0.49 ± 0.12 0.48 ± 0.12¶	62 70¶

Comparing various structural parameters and the paramyosin: myosin heavy chain molar ratios between tarantula and *Limulus* thick filaments.
* Number of measurements.
‡ Previously published (5).
§ Previously published (13).
¶ Previously published (19).

paramyosin on the basis of its having similar mobility to that of purified *Limulus* paramyosin (8, 21). In all cases where purified *Limulus* PM was added to homogenates of tarantula muscle the staining intensity of this band but no other was increased (Fig. 5). We previously reported (8, 21) that the paramyosin band on gels of homogenates of glycerinated muscle does not appear to undergo the type of proteolysis observed when molluscan paramyosin is freshly prepared. Nor do we see any indication of β or γ paramyosin breakdown products in our purified *Limulus* paramyosin.

In all gels a thin, weakly staining band precedes the paramyosin band but does not show increased staining intensity upon the addition of purified paramyosin. Thus, all of our measurements excluded the contribution of this lower molecular weight polypeptide. There is no difference in the appearance of the paramyosin band on disk or slab gels. We did not attempt further identification of the paramyosin band in tarantula gels.

Gels loaded with between 4.1 and 22.5 μg of total myofibrillar protein, respectively, give consistent "uncorrected" (dye binding) paramyosin:myosin heavy chain ratios for each of the two species. Thus, we are confident that, within the range of protein loadings used, Coomassie Brilliant Blue bound to these in direct proportion to their protein content. The "corrected" (21) molar ratios from a total of 62 individual gels were averaged to obtain the PM:MHC molar ratio of 0.49 $\pm$ 0.12 SD for *Limulus* thick filaments which is in excellent agreement with our previously reported ratio of 0.48 $\pm$ 0.12 SD (21). The values from 61 gels were averaged to obtain the PM:MHC molar ratio of 0.31 $\pm$ 0.079 SD for tarantula thick filaments. Thus, paramyosin accounts for 33% of the molecules of *Limulus* filaments but only 24% of the molecules of tarantula filaments (Table III).

DISCUSSION

Our images of fixed, sectioned tarantula femur muscles show the same structural organization earlier reported by Zebe and Rathmeyer (39) in their study of four different tarantula leg muscles, as well as by Sherman and Luff (29) for tarantula tarsal claw depressor muscle and Kawaguti and Kamishima (14) for other spider leg muscles. The contractile apparatus of spider muscle also resembles that of other long-sarcomere arthropod muscles, having narrow myofibrils with somewhat skewed sarcomeres, thick filaments organized into an irregular hexagonal lattice within the A-band, and 9–12 thin filaments surrounding each thick filament (4, 8, 21). Many such long-sarcomere muscles are highly extensible and undergo considerable changes in sarcomere length during isotonic contraction, in situ, which may involve alteration in filament organization. For example, at their longer lengths, the sarcomeres of *Limulus* telson and slow crustacean fibers frequently display A-bands with jagged boundaries due to misalignment of thick filaments (4, 19, 21). At the shortest in situ sarcomere-lengths barnacle thick filaments have been observed to penetrate the Z-bands and enter neighboring sarcomeres (23), while *Limulus* thick filaments have been reported to decrease in length (3–6). We have not yet determined whether or not such extensibility is a property of tarantula leg muscle. All of the fibers we examined were fixed at "body length" and show complete overlap of thick and thin filaments at a sarcomere length of $\sim$5.0 μm. Zebe and Rathmeyer (39) reported sarcomere lengths between 3.0 and 7.3 μm with A-bands between 2.8 and 5.6 μm for the tarantula leg muscles they examined. It is not clear, however, whether the variability they observed was present in separate muscles (as in the case of tarantula tarsal claw depressor vs. levator [18]) or even different fibers in the same muscle. *Heteropoda* leg muscle sarcomeres measure 5.3–5.5 μm when fixed slightly stretched. Thick filaments (up to 3.5 μm long) are misaligned, forming an irregular A-I boundary (14). Tarantula tarsal claw depressors have a mean sarcomere length of 6.2 μm with A-bands ranging from 4.0 to 5.2 μm (29). All of these spider muscles exhibit solid, rather than discontinuous, Z-bands, which might seem to preclude passage of thick filaments from one sarcomere to another at short sarcomere lengths. We have, however, seen some indication of just this phenomenon in rare instances, in tarantula fibers, in sarcomeres <4.0 μm in length. Spider sarcomeres have not yet been examined at their longest in situ length, but in the case of the tarantula femur muscles, if we assume a mean thick filament length of $\sim$4.5 μm and a mean thin filament length of $\sim$2.5 μm (we see no double overlap of thin filaments but also no H zone in 5 μm long sarcomeres), it is possible for sarcomeres to extend to slightly >9.0 μm and still retain filament overlap, without the necessity for gross misalignment of thick filaments within the A-bands. Additional, systematic studies must be done before we can describe the appearance of tarantula femur sarcomeres at different lengths.

When negatively stained and metal-shadowed thick filaments isolated from tarantula fibers are examined, one is aware of their striking resemblance to similarly prepared filaments isolated from *Limulus* muscle. Both electron microscope images of negatively stained tarantula filaments and the optical transforms obtained from these images demonstrate a highly ordered cross-bridge arrangement on the filaments' surfaces. Calculations, based on measurements of spacings on the diffraction patterns, strongly support a threefold screw symmetry and a rotational symmetry of four for the tarantula filaments. It should be noted that although we examined many tarantula filaments, we have analyzed the optical transforms from fewer of them (n = 16) than we originally did for *Limulus* filaments (n = 50) (15). Nevertheless, the values that we obtained are consistent, as can be seen by comparing the standard deviations of the measurements on diffraction patterns from tarantula filament images with those from *Limulus* (Tables I and II). In addition to their helical and rotational symmetries, there are other points of similarity between tarantula and *Limulus* thick filaments. The orientation and location of stain-excluding regions on optical reconstructions of tarantula filaments closely resemble the disposition of cross-bridges both on the computer-filtered image of negatively stained *Limulus* filaments and on a model for the arrangement of *Limulus* cross-bridges that we have generated from diffraction data (22, 30) (Fig. 4). Both unidirectionally metal-shadowed tarantula and *Limulus* filaments display a major right-handed surface helix which repeats axially every 43.5 nm. Both filaments also appear to have the same number of subunits arranged along each strand of this helix, which can be seen in fortuitously oriented specimens and optically filtered images of such specimens (16). For *Limulus*, we have been able to ascertain that each subunit represents the two S-1s from one myosin molecule, based on computer image analysis and stem mass measurements (R. J. C. Levine, Freeman, and W. Hofmann, unpublished results). Although we cannot determine whether this is the case for tarantula filaments as well, from the data reported here we believe that it is the most likely interpretation of subunit structure.

The structural similarities between tarantula and *Limulus* filaments seem quite remarkable, in view of the fact that the organization of cross-bridges on the surface of many other arthropod thick filaments is quite different. Wray (33–35) and Wray et al. (37) has reported helical repeats between 30 and 40 nm for a variety of insect and crustacean thick filaments from his x ray diffraction analyses, and in preliminary studies we observed similar periodicities, most likely arising from nonintegral surface helices, in optical transforms from negatively stained images of thick filaments isolated from such long-sarcomere arthropod muscles as insect leg (17) and lobster crusher claw (R. Kensler and R. J. C. Levine, unpublished observation). The similarity between tarantula and *Limulus* thick filaments may be explained on the basis of the close phylogenetic relationship between these species: both *Limulus* and the arachnids (of which tarantula is an example) belong to the chelicerate subphylum of the arthropod phylum. In support of a phylogenetic basis for this structural organization, preliminary examination of thick filaments isolated from muscles of another chelicerate arthropod: scorpion reveals that these also show a marked resemblance to those of *Limulus* and tarantula (17).

Despite the obvious and striking similarities in the arrangement of cross-bridges on their surfaces, there are differences between *Limulus* and tarantula thick filaments, most prominently with respect to paramyosin content and filament diameter. These may be related, although in an earlier study we found that for the muscles examined the paramyosin content was directly proportional to filament length, not diameter (21). Surprisingly, although tarantula thick filaments are as long as those isolated from unstimulated *Limulus* muscle, they contain ~9% fewer paramyosin molecules than the latter. We are confident that the value we have obtained for the paramyosin content of tarantula filaments is correct, since we simultaneously obtained a PM:MHC molecular ratio for *Limulus* thick filaments which was virtually identical to that we reported several years ago (21).

The role of paramyosin, which occupies the core of most invertebrate thick filaments, is not well understood, other than as "scaffolding" upon which a cortical layer of myosin molecules aggregates in order to form thick filaments >1.6 μm in length. This has been reported for synthetic filaments of horseshoe crab myosin and paramyosin (13) and for in situ thick filaments of nematode mutants that lack paramyosin (24). Cohen (2) has recently suggested that paramyosin affects filament assembly only in the case of the thick filaments of molluscan catch muscles, which have extraordinarily large amounts of this protein (75–80%) relative to myosin. Epstein et al. (9), however, reported that molluscan paramyosin decreases the affinity of both molluscan and rabbit myosin for F actin in vitro, indicating a specific biochemical interaction between the two thick-filament proteins.

A possible structural reflection of paramyosin content of thick filaments is a difference in the appearance of their core and cortical regions (2). Fly muscle, which has relatively little paramyosin (1, 28), has noticeably "hollow"-appearing thick filaments (25, 28), while the thick filaments of *Lethocerus* flight muscle contain more paramyosin (1, 20) and appear more "solid," although they do display core regions which stain different than the cortices, particularly when tannic acid is included in the fixative (25). Our electron micrographs of cross-sectioned tarantula fibers fixed in the presence of tannic acid show filaments with core regions that stain less intensely than does the periphery, but the filaments do not usually appear "hollow." *Limulus* filaments appear even more "solid" (4). The longitudinal striping which is seen much more clearly on negatively stained tarantula thick filaments than on those of *Limulus* may reflect the organization of myosin tails or subunits composed of several myosin tails. The prominence of these structures on the tarantula filaments may be due to their lesser content of paramyosin, which does not obscure their presence.

We found that tarantula femur thick filaments have smaller diameters than those of *Limulus* muscle, from analysis of measurements made of cross-sectioned filament profiles in intact fibers and in the bare-zone regions of negatively stained isolated filaments on high power electron micrographs. Earlier reports have given tarantula thick-filament diameters from as small as 15 nm to as large as 23.5 nm (29, 39). All of the previous measurements were made on several thick-filament profiles in cross-section only and were not analyzed statistically nor supported by independent measurements by another technique. *Limulus* thick filaments have been shown to have a diameter of 23.5 nm by a variety of techniques (3, 15, 30). The smaller diameter of tarantula filaments (~20 nm) that we demonstrated by electron microscopy can also be deduced from optical transforms obtained from images of negatively stained isolated filaments. In the tarantula diffraction patterns, the reflections which are governed wholly or in part by the radius of the centers of mass of the cross-bridges: the subsidiary maxima on the 1/14.5 nm^{-1} meridional reflection and the primary maxima on the first and fourth layer lines (12, 37) are radially positioned farther away from the meridian than is the case on transforms obtained from *Limulus* filaments. While this is consistent with a smaller diameter for the tarantula filaments, it also may indicate that they have a more ordered surface lattice than do *Limulus* filaments. A transition from a less ordered to a more ordered cross-bridge array has been reported for glycerinated, relaxed *Limulus* fibers exposed to solutions of decreasing ionic strength by Wray et al. (36).

The actual orientation of surface subunits and number of myosin cross-bridges/subunit on tarantula thick filaments, however, cannot be established with certainty until computer image reconstructions are available (30, 31). Nevertheless, based on our measurements of the diameter of the filament backbone, the centers of mass of the subunits lie close to 4 nm from the tarantula filament shift, as they do in *Limulus* thick filaments. We have previously shown that the centers of mass occur at this radius in *Limulus* filaments because the cross-bridges, each composed of the two S-1s of a single myosin molecule (8-nm diameter × ~20 nm length), are tilted azimuthally so that their long axes lie nearly tangential to the circle describing the filament backbone (30). The similarity of the distance of the cross-bridge mass from the surfaces of the two filaments, as well as the resemblance between optically filtered images of tarantula filaments (Fig. 4) and the computer-filtered one of the *Limulus* filaments (30), suggests a comparable orientation of cross-bridges on both. If this interpretation is confirmed by computer reconstruction of the tarantula filament, any differences in the orderliness of the cross-bridge array that may exist among the chelicerate thick filaments may indeed result from very subtle structural variations.

As mentioned above, it is unlikely that the smaller diameter of tarantula thick filaments (vs. *Limulus*) is related to the

lesser paramyosin content of the former, since a relationship between filament diameter and paramyosin content does not hold over a variety of thick filaments from invertebrate striated muscles (21). For example, the thick filaments of scallop striated adductors have much less paramyosin (~16% of total molecules) (21) than those of either tarantula or *Limulus* muscle, yet both the mollusc and arthropod filaments have comparable diameters (21, 31). The scallop filaments most likely have a greater portion of their volume occupied by myosin rods than arthropod filaments do, since three-dimensional reconstructions indicate that the former possess seven, not four, myosin cross-bridges per crown (31).

Since the evidence suggests that the amount of paramyosin present probably does not influence the packing of surface myosin molecules in the chelicerate arthropod filaments we have studied, it is interesting that myosin aggregates to form the cortical layers of filaments with different diameters but with almost, if not actually, identical cross-bridge arrays, as seen in these muscles. Studies underway on the structure of synthetic filaments formed from chelicerate myosin alone and comparative analysis of the properties of myosins of the different chelicerate muscles may clarify this finding.

Of even greater significance is the usefulness of the chelicerate thick filaments as models in experiments designed to examine cross-bridge movement during muscle contraction. Since the structure of these filaments in the "relaxed" state is both ordered and well-defined, interpretation of any changes in cross-bridge orientation associated with changing environmental conditions such as ATP depletion, divalent cation concentration or variations in ionic strength should be both fairly straightforward and highly informative. We are currently pursuing this line of research.

We wish to thank Dr. John Wray for much helpful discussion. We gratefully acknowledge the secretarial assistance of Dolores Wells.

This work was supported in part by U. S. Public Health Service grants: HL15835 to the Pennsylvania Muscle Institute, GM 07475, AM 30442, AM 14317, and Projekt GO 28414-7 from the Federal Republic of Germany.

A preliminary report of portions of this work was presented at the Biophysical Society meeting, February, 1982 (17).

Received for publication 12 November 1982, and in revised form 11 March 1983.

Note Added in Proof. Preliminary results on computer image of tarantula filaments were recently reported by A. Crowley, R. Padron, and R. Craig.

REFERENCES

1. Bullard, B., B. Luke, and L. Winkelman. 1973. The paramyosin of insect flight muscle. *J. Mol. Biol.* 75:359–367.
2. Cohen, C. 1982. Matching molecules in the cach mechanism. *Proc. Natl. Acad. Sci. USA.* 79:3176–3178.
3. Dewey, M. M., D. Colflesh, P. Brink, S. F. Fan, and B. Gaylinn. 1982. Structural function and chemical changes in the contractile apparatus of *Limulus* striated muscle as a function of sarcomere shortening and tension development. *In* Basic Biology of Muscle: A Comparative Approach. B. M. Twarog, R. J. C. Levine, M. M. Dewey, editors. Raven Press, New York. 53–72.
4. Dewey, M. M., R. J. C. Levine, and D. E. Colflesh. 1973. Structure of the telson muscules of *Limulus*. The contractile apparatus at various sarcomere lengths. *J. Cell Biol.* 58:574–593.
5. Dewey, M. M., R. J. C. Levine, B. Walcott, L. Brann, A. Baldwin, and P. Brink. 1979. Structural changes in thick filaments during sarcomere shortening in *Limulus* striated muscle. *In* Cross-bridge Mechanism in Muscle Contraction. H. Sugi and G. H. Pollack, editors. University of Tokyo Press, Tokyo. 3–22.
6. Dewey, M. M., B. Walcott, D. E. Colflesh, H. Terry, and R. J. C. Levine. 1977. Changes in thick filament length in *Limulus* striated muscle. *J. Cell Biol.* 75:366–380.
7. Dillon, L. S. 1952. The myology of the aranied leg. *J. Morphol.* 90:467–480.
8. Elfvin, M., R. J. C. Levine, and M. M. Dewey. 1976. Paramyosin in invertebrate muscles. I. Identification and localization. *J. Cell Biol.* 71:261–272.
9. Epstein, H. F., B. J. Aronow, and H. E. Harris. 1976. Myosin-paramyosin cofilaments: enzymatic interactions with F-actin *Proc. Natl. Acad. Sci. USA.* 76:3015–3019.
10. Erickson, H. P., W. Voter, and K. Leonard. 1978. Image reconstruction: enhancement of periodic structure by optical filtering. *Methods Enzymol.* 49:39–63.
11. Gregory, D., and B. J. S. Pirie. 1973. Wetting agents for biological electron microscopy I. General considerations and negative staining. *J. Microcs. (Lond.).* 99:251–265.
12. Haselgrove, J. C. 1980. A model of myosin cross-bridge structure consistent with the low-angle X-ray diffraction pattern of vertebrate muscle. *J. Muscle Res. Cell Motil.* 1:177–191.
13. Ikemoto, N., and S. Kawaguti. 1967. Elongating effect of tropomyosin A on thick filaments in the long sarcomere muscle of the horseshoe crab. *Proc. Jpn. Acad.* 43:974–979.
14. Kawaguti, S., and Y. Kamishima. 1969. Electron microscopy on the long-sarcomere muscle of the spider leg. *Biol. J. Okayama Univ.* 15:73–86.
15. Kensler, R. W., and R. J. C. Levine. 1982. An electron microscopic and optical diffraction analysis of the structure of *Limulus* telson muscle thick filaments. *J. Cell Biol.* 92:443–451.
16. Kensler, R. W., and R. J. C. Levine. 1982. Determination of the hand of the cross-bridge helix of *Limulus* thick filaments. *J. Muscle Res. Cell Motil.* 3:349–361.
17. Kensler, R. W., R. J. C. Levine, M. Reedy, and W. Hofmann. 1982. Arthropod thick filament structure. *Biophys. J.* 37:34a. (Abstr.)
18. Laemmli, U. K. 1970. Cleavage of structural proteins during the assembly of the head of bacteriophage T_4. *Nature (Lond.).* 227:680–685.
19. Levine, R. J. C., M. M. Dewey, and G. W. deVillafrance. 1972. Immunohistochemical localization of contractile proteins in *Limulus* striated muscle. *J. Cell Biol.* 55:221–235.
20. Levine, R. J. C., M. M. Dewey, M. Elfvin, and B. Walcott. 1974. *Lethocerus* flight muscle paramyosin: antibody localization and electrophoretic studies. *Am. J. Anat.* 141:453–458.
21. Levine, R. J. C., M. Elfvin, M. M. Dewey, and B. Walcott. 1976. Paramyosin in invertebrate muscles. II. Content in relation to structure and function. *J. Cell Biol.* 71:273–279.
22. Levine, R. J. C., R. W. Kensler, M. Stewart, and J. C. Haselgrove. 1982. The molecular organization of *Limulus* thick filaments. *In* Basic Biology of Muscle: A Comparative Approach. B. M. Twarog, R. J. C. Levine, and M. M. Dewey, editor. Raven Press, New York. 37–52.
23. Leyton, R. A., and W. C. Ullrick. 1970. Z disc ultrastructure in several depressor fibers of the barnacle. *Science (Wash. DC).* 168:127–128.
24. Mackenzie, J. M., Jr., and H. F. Epstein. 1980. Paramyosin is necessary for determination of Nematode thick filament length *in vivo*. *Cell.* 22:747–755.
25. Reedy, M. C., M. K. Reedy, and R. Goody. 1983. Coordinated electron microscope and x-ray studies of glycerinated insect flight muscle. II. Electron microscopy and image reconstruction of muscle fibers fixed in rigor, in ATP and in AMPPNP. *J. Muscle Res. Cell Motil.* In press.
26. Reedy, M. K. 1967. Cross-bridges and periods in insect flight muscle. *Am. Zool.* 7:465–481.
27. Reedy, M. K. 1968. Ultrastructure of insect flight muscles. I. Screw sense and structural grouping in the rigor cross-bridge lattice. *J. Mol. Biol.* 31:155–176.
28. Reedy, M. K., K. R. Leonard, R. Freeman, and T. Arad. 1981. Thick myofilament mass determination by electron scattering measurements with the scanning transmission electron microscopic *J. Muscle Res. Cell Motil.* 2:45–64.
29. Sherman, R. G., and A. R. Luff. 1971. Structural features of the tarsal claw muscles of the spider *Eurypelma marxi* Simon. *Can. J. Zool.* 49:1549–1556.
30. Stewart, M., R. W. Kensler, and R. J. C. Levine. 1981. Structure of *Limulus* telson muscle thick filaments. *J. Mol. Biol.* 153:781–790.
31. Vibert, P., and R. Craig. 1982. Three-dimensional reconstruction of scallop thick filaments. *Biophys. J.* 37:266a. (Abstr.)
32. Weber, K., and M. Osborn. 1969. The reliability of molecular weight determinations by dodecyl-sulfate polyacrylamide gel electrophoresis. *J. Biol. Chem.* 244:4406–4412.
33. Wray, J. S. 1979. Structure of the backbone in myosin filaments of muscle. *Nature (Lond.).* 277:37–40.
34. Wray, J. S. 1979. X-ray diffraction studies of myosin filament structures in crustacean muscles. *In* Motility in Cell Function. F. A. Pepe, J. W. Sanger, and V. T. Nachmias, editors. Academic Press, Inc., New York. 347–350.
35. Wray, J. S. 1982. Organization of myosin in invertebrate thick filaments. *In* Basic Biology of Muscle: A Comparative Approach. Ed. B. M. Twarog, R. J. C. Levine, and M. M. Dewey, editors. Raven Press, New York 29–36.
36. Wray, J. S., P. J. Vibert, and C. Cohen. 1974. Crossbridge arrangements in *Limulus* muscle. *J. Mol. Biol.* 88:343–348.
37. Wray, J. S., P. J. Vibert, and C. Cohen. 1975. Diversity of crossbridge arrangements in invertebrate muscles. *Nature (Lond.).* 257:561–564.
38. Wrigley, N. G. 1968. The lattice spacing of crystalline catalase as an internal standard of length in electron microscopy. *J. Ultrastruct. Res.* 24:454–464.
39. Zebe, E., and W. Rathmeyer. 1968. Electronenmikroskopische Untersuchungen an Spinnenmuskeln. *Z. Zellforsch. Mikros. Anat.* 92:377–387.